

Electro-optically tunable single-frequency lasing from neodymium-doped lithium niobate microresonators

Yannick Minet,^{1,2,*} Simon J. Herr,³ Ingo
Breunig,^{1,3,†} Hans Zappe,² and Karsten Buse^{1,3}

¹*Laboratory for Optical Systems,*

*Department of Microsystems Engineering - IMTEK, University of Freiburg,
Georges-Köhler-Allee 102, 79110 Freiburg, Germany*

²*Gisela and Erwin Sick Chair of Micro-Optics,*

*Department of Microsystems Engineering - IMTEK, University of Freiburg,
Georges-Köhler-Allee 102, 79110 Freiburg, Germany*

³*Fraunhofer Institute for Physical Measurement Techniques IPM,
Georges-Köhler-Allee 301, 79110 Freiburg, Germany*

(Dated: May 9, 2022)

Abstract

Tunable light sources are a key enabling technology for many applications such as ranging, spectroscopy, optical coherence tomography, digital imaging and interferometry. For miniaturized laser devices, whispering gallery resonator lasers are a well-suited platform, offering low thresholds and small linewidths, however, many realizations suffer from the lack of reliable tuning. Rare-earth ion-doped lithium niobate offers a way to solve this issue. Here we present a single-frequency laser based on a neodymium-doped lithium niobate whispering gallery mode resonator that is tuned via the linear electro-optic effect. Using a special geometry, we suppress higher-order transverse modes and hence ensure single-mode operation. With an applied voltage of just 68 V, we achieve a tuning range of 3.5 GHz. The lasing frequency can also be modulated with a triangular control signal. The freely running system provides a frequency and power stability of better than $\Delta\nu = 20$ MHz and 6 %, respectively, for a 30 minute period. This concept is suitable for full integration with existing photonic platforms based on lithium niobate.

I. INTRODUCTION

There is a strong demand for miniaturized, tunable lasers providing stable single-frequency lasing plus fast and wide tuning. Optical microresonators offer a possibility to accomplish this task since it is possible to fabricate them on on-chip material platforms. These microresonators are characterized by a high quality factor (Q -factor) and a small mode volume. They can be fabricated with a large free spectral range, in the best case with only one resonator mode in the whole gain bandwidth of the laser medium. Additionally, they provide the possibility of designing the

* yannick.minet@imtek.uni-freiburg.de

† ingo.breunig@ipm.fraunhofer.de

transvers mode spectrum which ensures single-mode lasing.

These properties can be used to passively stabilize lasers via self-injection locking [1–4]. In Ref. [3], a compact on-chip system with a small linewidth was realized. It can be linearly tuned as fast as 12 PHz s^{-1} . However, the tuning range of the system is limited by the locking bandwidth of the external resonator to the laser chip, which is about 1 GHz. In contrast to the self-injection technique, it is also possible to generate laser light directly from microresonators fabricated out of active laser media. The properties of microresonator described in the introduction before enable a low pump threshold and narrow linewidth. Such systems have been proposed and demonstrated in a large variety of material platforms [5, 6]. For example, ultra-low threshold lasing of a titanium doped sapphire whispering gallery laser has been shown recently [7].

Whereas single frequency operation and wafer-scale fabrication in most systems is possible, changing the laser frequency often remains challenging. While approaches like temperature tuning or mechanical stress can achieve response times in the millisecond or microsecond range, linear electro-optic tuning offers even faster performance [8, 9]. Lithium niobate (LN), as a non-centro-symmetric crystal, offers the possibility of influencing the refractive index n by the linear electro-optic effect, the Pockels effect. In addition, large non-linear coefficients and a wide transparency range make LN an attractive material for many applications [10–13].

Additionally, rare-earth doped lithium niobate can serve as a laser material platform. A wide range of active components has been experimentally demonstrated on this platform, such as amplifiers and lasers [14–20]. The outstanding optical performance as well as the possibility of doping LN makes it a promising candidate to realize monolithic tunable laser sources. In Ref. [18] an electro-optically tunable erbium-doped lithium niobate microring laser has been demonstrated. However, the laser possesses multi-mode operation during the tuning and the electro-optical tuning efficiency suffers from the small spatial overlap between the optical mode and

the electric control field. Furthermore, the electro-optic tuning behavior of such a microresonator laser has never been analyzed in detail.

In this work, we demonstrate an electro-optically tunable single-frequency laser based on a neodymium-doped lithium niobate microresonator. Using a four-level system as provided by the trivalent neodymium ions has the advantage of leading to a far lower lasing threshold compared with that of a three-level system. In order to ensure a high excitation efficiency we resonantly pump the whispering-gallery resonator (WGR). Using extraordinarily polarized light, i.e. polarized parallel to the c -axis, has two advantages: Firstly, the absorption cross-section of the Nd-ions for the pump light is higher than that for ordinarily polarized light [21], resulting in a more efficient excitation scheme. Secondly, for electro-optic tuning of the lasing frequency we can make use of the Pockels coefficient r_{33} which is in our case the largest accessible electro-optic (EO) coefficient of lithium niobate, requiring lower voltages.

To ensure single-mode operation, we make use of a so-called photonic belt resonator geometry, which suppresses higher-order transverse modes [22]. By this micrometer-sized structure, we can also prevent undesired self-frequency doubling given by fortuitous phase-matching with higher order modes [23]. In the following, we first elucidate the theoretical quantities such as the pump threshold and the influence of the Pockels effect on the resonance frequency. Then, we experimentally verify the single-frequency operation and analyze the stability of the laser. Finally the tuning of this laser light source is demonstrated.

II. THEORETICAL CONSIDERATIONS

The threshold power P_{th} for lasing in a microresonator can be determined by [24],

$$P_{\text{th}} = \frac{2\pi n_1 h c_0 V_p}{\lambda_l \lambda_p Q_l \sigma_{\text{em}} \tau \eta} \quad (1)$$

with the refractive index at the lasing wavelength n_1 , the mode volume of the pump mode V_p , the lasing wavelength λ_l , the pump wavelength λ_p , the quality factor at the lasing wavelength Q_l , the emission cross section σ_{em} , the lifetime τ and the excitation efficiency η . In Ref. [24] η was derived for a non-resonant pump scheme. We will in the following deduce η for our resonant pump scheme. The parameter η is defined as the fraction of the absorbed pump power in order to pump the laser process P_{abs} over the total pump power P as

$$\eta = \frac{P_{\text{abs}}}{P} = \frac{P_{\text{int}}}{P} (1 - e^{-\alpha L}) \quad (2)$$

with the absorption coefficient α , the path length $L = 2\pi R$, the radius R and the internal power P_{int} . We assume that absorption is the dominant loss at the pump wavelength and every absorbed photon leads to the excitation of the upper laser level. Furthermore, we use the a first order approximation for $e^{-\alpha L} \approx 1 - \alpha L$. Expressing the resonant power enhancement P_{abs}/P by the intrinsic finesse of the resonator \mathcal{F}_{int} and the coupling efficiency K , Eq. (2) reads as

$$\eta = \frac{\mathcal{F}_{\text{int}}}{2\pi} K \alpha L \quad (3)$$

Assuming that the pump light is non-detuned from the resonance of the pump mode and inserting the intrinsic finesse as $\mathcal{F}_{\text{int}} = 2\pi/\alpha L$ into Eq. (3), we obtain :

$$\eta = K \quad (4)$$

Consequently, the highest excitation efficiency and therefore the lowest threshold is observed in critical coupling with $K = 1$.

Let us consider e-polarized pump light with $\lambda_p = 813$ nm. With $\sigma_{\text{em}} = 1.8 \times 10^{-19}$ cm² [21], $\tau = 100$ μ s, $V_p = 10^6$ μ m³, $n = 2.15$, $Q_1 = 6 \times 10^6$ and $\eta = 1$ we obtain $P_{\text{th}} \approx 0.3$ mW.

We can also estimate the introduced shift of the lasing frequency ν_1 by an external electric field E_z . The resonance frequency of the WGR, being identical with the possible laser frequency ν_1 , can be estimated by [25]

$$\nu_1 \approx m \frac{c}{2\pi R n_1} \quad (5)$$

for the major radius of the microresonator R , the azimuthal mode number m , the vacuum speed of light c and the refractive index of the bulk material n_1 at the lasing wavelength.

From Eq. (5) it is clear that either changing the radius R or the refractive index n_1 will change the eigenfrequency. Since lithium niobate possesses the Pockels effect, the lasing frequency can be changed by applying an external voltage to the crystal. The refractive index is modified according to

$$\Delta n_1 = -\frac{1}{2} n_1^3 r E_z. \quad (6)$$

for r the Pockels coefficient and $E_z = U_c/d$ the electric field resulting from the control

voltage U_c divided by the thickness d of the WGR. Combining Eqs. (5) and (6), the change of the eigenfrequency $\Delta\nu_1$ can then be expressed as

$$\Delta\nu_1 = \frac{1}{2}n_1^2rE_z\nu_1. \quad (7)$$

We neglect the contribution of the piezo-electric effect to the frequency change since it is an order of magnitude smaller than the Pockels effect [26]. Using Eq. (7) we can make an estimate for the expected frequency tuning range. Assuming $U_c = 62.5\text{ V}$ and a thickness d of $250\text{ }\mu\text{m}$ which results in a electric field strength of $E = 250\text{ V mm}^{-1}$, a Pockels coefficient $r_{33} = 25\text{ pm V}^{-1}$ [27] and a lasing frequency of $\nu_1 = 276.15\text{ THz}$, we determine the frequency shift to be $\Delta\nu \approx 4.0\text{ GHz}$. Since we employ a special, wedge-like geometry (Fig. 1 a)) we need to consider a reduction of the electric field compared of that of a simple plate capacitor. It has been shown before, that the overlap between the externally applied electric field and the optical electric field is reduced depending on the size of the belt [28]. A drop of about 50% for larger sizes of the wedge is expected. Additionally, with larger sizes the homogeneity of the electric control field decreases. However, a small size of wedge is desired to suppress higher-order modes and therefore ensure single mode lasing and suppress undesired self-frequency doubling [23].

III. EXPERIMENTAL METHODS

The microresonator was fabricated from a commercially available single-domain congruent z -cut lithium niobate (LiNbO_3) wafer of $250\text{ }\mu\text{m}$ doped with nominally 0.4 mol% neodymium (Nd) and 5.1 mol% magnesium oxide (MgO) (Yamaju Ceramics Co. Ltd.). To provide a low resistance electrical connection, the $+z$ and $-z$ -sides of the wafer are coated with a 250-nm-chrome layer. To cut a resonator blank out of

the wafer, we use a femtosecond laser with a repetition rate of 60 kHz and a wavelength of 343 nm. The average power was 1 W. To ensure a sufficient mechanical and electrical connection, the crystal blank is soldered to a brass post using low temperature soldering tin.

Then, using the same femtosecond laser, we shape the resonator using a computer-controlled lathe. The WGR has a major radius $R = 800 \mu\text{m}$, resulting in a free spectral range (FSR) of 27.1 GHz. The optic axis is parallel to the axis of symmetry of the resonator. The wedge-like geometry, shown in Fig. 1 a), has a base B of $7.5 \mu\text{m}$ and a height H of $5 \mu\text{m}$. In the final step of the machining in order to improve the quality factor of the resonator, a single run of 2 min chemical mechanical polishing is done. As shown in Fig. 1 b), after polishing, the previously manufactured corners of the wedge are slightly rounded off.

The setup for the optical characterization consists of a pump laser, coupling optics and mechanics, a voltage source for the tuning, a protective housing and devices to characterize the properties of the emitted beam (Fig. 1 c)). As a pump laser we use either a titanium sapphire laser or a 813-nm single frequency laser diode. While both lasers are used for characterization, only the Ti:Sa laser is used as a pump laser in the electro-optical tuning experiments. The extraordinarily polarized pump beam is coupled resonantly into the resonator via a rutile prism.

The residual pump light and the generated laser light are separated using a dichroic mirror and sent to a beam dump. The generated laser light is split into two arms to be further analyzed either using a scanning Fabry-Pérot-Interferometer (FPI) or an optical spectrum analyzer (OSA). The FPI has a FSR of 1.5 GHz and is scanned by multiple FSRs during the experiment. The linewidth of the FPI is 10 MHz. The OSA (Yokogawa AQ6370D) is used to measure the absolute frequency and to resolve a larger frequency range. It has a resolution of 15 GHz. To maintain similar conditions for all experiments, the WGR is housed in an acrylic glass cover.

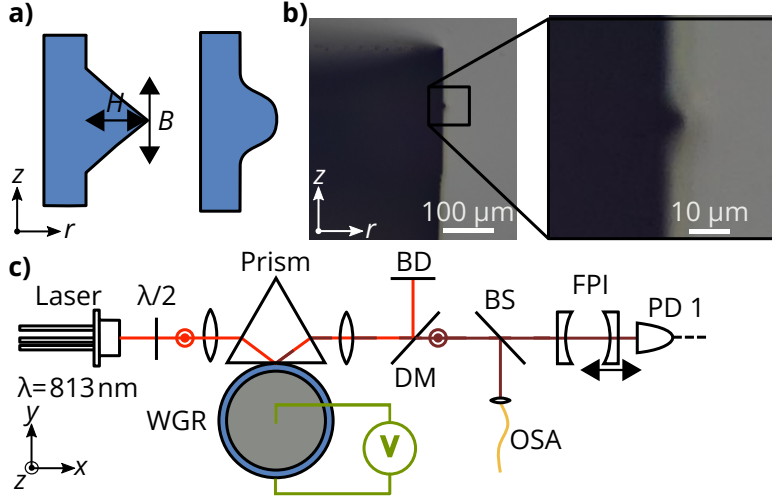


FIG. 1. **a)** Drawing of the resonator with the corresponding coordinates of the base B and the height H after laser cutting (left) and polishing (right). **b)** Microscopic side view of the fabricated wedge-like structure of the resonator after polishing. **c)** A schematic of the measurement setup. The laser with $\lambda_1 = 813 \text{ nm}$ is coupled via a rutile prism to the whispering gallery resonator (WGR). The polarization is controlled by a $\lambda/2$ -wave-plate. The remaining pump light is filtered using a dichroic mirror (DM) and sent to a beam dump (BD). The lasing beam is split by a 50:50 beam splitter (BS) and further analyzed using a scanning Fabry-Pérot-Interferometer (FPI) and an optical spectrum analyzer (OSA).

Measurements begin after a period of a few minutes to allow the system to attain thermal stability, since no temperature controller is active for the experiments. For the electro-optic control of the resonance frequency a copper wire is bonded onto the top of the WGR while the bottom is connected to the brass post. The control signal from the function generator is amplified by a 10 volt-per-volt high-voltage amplifier with a maximum output of 150 V. Using this setup, we measure the linewidth the WGR at $\lambda = 813 \text{ nm}$ as well as close to the expected lasing wavelength; the derived quality factors at pump and lasing wavelengths are $Q_p = 3 \times 10^5$ and $Q_l = 6 \times 10^6$, respectively. From a spectroscopic measurement we determine an absorbance of 0.6 cm^{-1} at $\lambda = 813 \text{ nm}$. The resulting intrinsic quality factor based on this value is

$$Q = 2.8 \times 10^5.$$

IV. RESULTS AND DISCUSSION

When the resonator is excited with extra-ordinarily polarized light at only $P_p = (4.0 \pm 0.5)$ mW laser excitation is clearly visible and emission of 1086 nm wavelength light is observed in both emission directions. This power value is higher than the estimated before, the difference stemming mainly from the unknown prism-to-resonator coupling strength during the laser operation.

As can be seen in Fig. 2 a) we observe only a single emission peak at the expected frequency $\nu_1 = 276.15$ THz; the entire measurement covers a frequency range of 450 GHz. The peak position corresponds to $\lambda_1 = 1085.6$ nm.

For higher spectral resolution we launch the generated laser light into the scanning FPI. The recorded spectrum can be seen in Fig. 2 b). Since only one peak is visible in the free spectral range, added to the fact that we scan over the entire 430-GHz gain bandwidth of Nd:MgO:LN [29], we verify single frequency operation. By fitting a Lorentzian function to the transmission peak, we determine a linewidth of the transmitted laser light similar to the linewidth of the FPI of 10 MHz, indicating that the measurement is equipment-limited.

The inset in Fig. 2 b) shows a false-color image of the beam profile, taken after collimating the beam with a 40-mm bi-convex lens. It shows a TEM₀₀-like shape, another clear indication of single mode operation.

For measurement of power and frequency stability, an additional beam splitter and a photodiode are placed in front of the FPI. First, we couple about 12 mW of pump light into the resonator, leading to a lasing power of $P_l = 340$ μ W. The result is shown in Fig. 3 where the upper part shows the frequency stability and the lower one, the power stability for a 30 min period. The lasing frequency ν_1 shows a drift

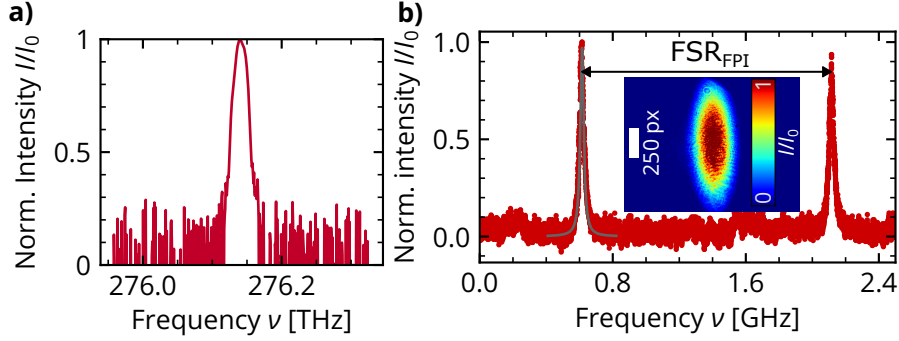


FIG. 2. Characterization of the emitted laser light. **a)** The recorded spectra of the optical spectrum analyzer (OSA) and in **b)** of the scanning Fabry-Pérot-Interferometer (FPI). The inset in **b)** shows a false-color picture recorded with a beam profile camera.

of about 20 MHz and the output power of the laser fluctuates within $\pm 6\%$ with a slight downward slope. Since the setup is not actively temperature stabilized, we assume that the frequency drift is caused by a change of the ambient temperature.

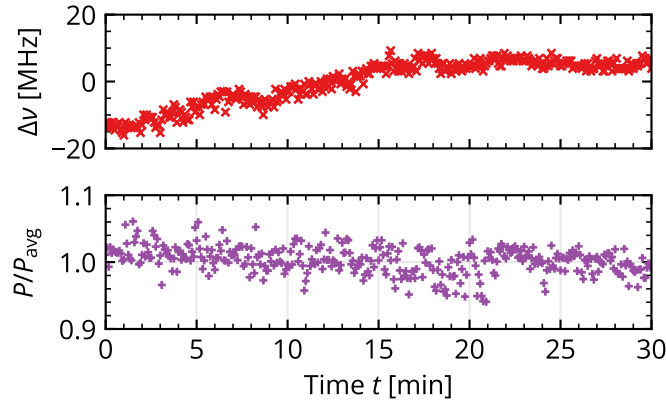


FIG. 3. Stability of the emission frequency and power of the free running system. The frequency was recorded by tracking the peak position of the scanning Fabry-Pérot-Interferometer (FPI). The power of the lasing is measured using an additional photodiode placed behind a 50:50 beam splitter in front of the FPI.

To demonstrate wavelength tuning, we apply a voltage that increases linearly in 10s to a maximum value of 70 V. Such a slow ramp ensures that the resonator can

thermalize at the in-coupled power and therefore remains in thermal equilibrium. The shift in peak position on the scanning FPI while increasing the voltage results in a measure for the change of the lasing frequency ν_1 as shown in Fig. 4). The maximum frequency shift we could obtain was 3.5 GHz. If we increase the voltage further we cannot observe lasing anymore. It is likely that the pump mode frequency is then shifted so far from resonance that we decouple the resonator from the pump light.

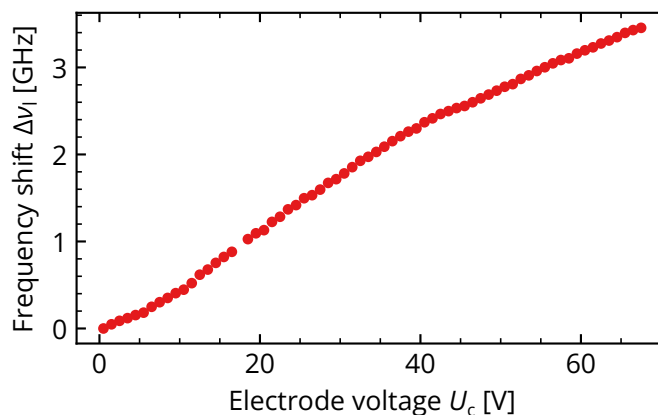


FIG. 4. Electro-optic tuning of the WGR-laser: Frequency shift $\Delta\nu_1$ of lasing frequency vs. applied voltage.

The magnitude of the observed lasing frequency shift corresponds to the GHz-broad resonances of the WGR, due to the strong absorption of the pump light. We observe a non-linear tuning behavior with increasing voltage. As we use a pump power of several mW, it is likely that thermal effects influence the frequency tuning characteristic. A change of the resonator temperature of just 10 mK leads to change of the resonance frequency $\Delta\nu \approx 100$ MHz [30]. Further investigations are needed to understand the origin of this nonlinearity.

The frequency shift amounts 3.5 GHz at 67.5 V. This is lower than the theoretically expected value of 4.3 GHz if the full electric field would be present. However,

a reduction is expected because of the wedge-like geometry of the resonator [28] and if we assume a reasonable reduction of 15 %, the theoretical value matches the experimentally measured one.

Finally, we quantify the tunability of the presented system for smaller tuning ranges but for higher tuning speeds. To do so, we apply a triangular voltage sweep to the resonator with a frequency of 11.25 Hz. The electric control signal and the resulting frequency shift can be seen in Fig. 5). By applying 15 V to the electrode we observe a frequency shift $\Delta\nu = 0.85$ GHz on the rising side resulting in a tuning rate of 57 MHz V^{-1} . On the rising side of the first triangle we extract from the linear fit $R^2 = 0.99$ and on the falling side $R^2 = 0.95$, indicating a high linearity of the observed frequency shift.

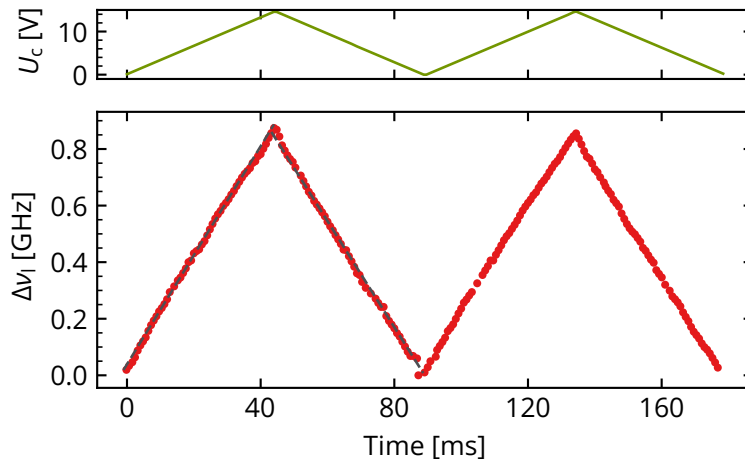


FIG. 5. Electro-optic tuning of the WGR-laser on the millisecond time scale. In the top plot we show the applied control voltage U_c on the electrodes. In the bottom the recorded frequency shift $\Delta\nu_l$ is displayed. The dash-dotted lines are linear fits to the recorded data.

V. CONCLUSION AND OUTLOOK

In summary, we implement an electro-optically tunable laser based on a Nd:Mg:LN microresonator, showing stable single-frequency lasing centered around 1086 nm wavelength with a TEM₀₀-like beam profile. The lasing frequency can subsequently be tuned more than 3.5 GHz without mode-hops. This free-running WGR laser provides 6 % output power stability as well as 20 MHz frequency stability without any feedback system for a period of 30 min. We have also demonstrated that using a triangular control signal leads to a corresponding linear shift of the lasing frequency, making the system useful as a possible light source for ranging and sensing, for example.

Since lithium niobate can be doped with other rare-earth ions such as praseodymium, tunable lasing could also be realized at visible wavelengths

A limitation of our demonstration is that resonant pumping limits the stable tuning range to the width of the pump mode. Furthermore, resonant pumping affects the tuning behavior, because less light is coupled into the resonator when a voltage is applied, which leads to a reduction in temperature and is most likely the origin of the nonlinear tuning behavior when the lasing frequency is tuned wide and slowly. One approach to tackle this issue is to employ a side-pumping scheme [31]. By doing so, even an inexpensive pump source like a 813-nm multi-mode laser diode can be employed. This ensures that the same pump power is always present during the electro-optic tuning. However, the quality factors achieved here were too low to use these schemes efficiently. Realizing this approach on an on-chip platform would push another limit: a smaller radius would lead to a larger FSR and hence larger tuning ranges would not be impeded by mode-hops, when only one longitudinal mode is present in complete gain bandwidth of the laser material [31]. Furthermore, by implementing this scheme in integrated photonic platforms based on lithium niobate

will lead to an increase of the electric field strength using the same voltage as used in this demonstration by two orders of magnitude and thus will allow for wider tuning - we consider this work to be an important step towards inexpensive tunable light sources.

ACKNOWLEDGMENTS

Y.M. acknowledges financial support by a Gisela and Erwin Sick Fellowship. The authors thank Jan Szabados and Nicolas Amiune for fruitful discussions on the manuscript.

-
- [1] V.V. Vassiliev, V.L. Velichansky, V.S. Ilchenko, M.L. Gorodetsky, L. Hollberg, and A.V. Yarovitsky. Narrow-line-width diode laser with a high- Q microsphere resonator. *Optics Communications*, 158(1):305–312, 1998.
 - [2] B. Sprenger, H. G. L. Schwefel, and L. J. Wang. Whispering-gallery-mode-resonator-stabilized narrow-linewidth fiber loop laser. *Opt. Lett.*, 34(21):3370–3372, Nov 2009.
 - [3] Viacheslav Snigirev, Annina Riedhauser, Grigory Lihachev, Johann Riemensberger, Rui Ning Wang, Charles Moehl, Mikhail Churaev, Anat Siddharth, Guanhao Huang, Yuri Popoff, et al. Ultrafast tunable lasers using lithium niobate integrated photonics. *arXiv preprint arXiv:2112.02036*, 2021.
 - [4] Mingxiao Li, Lin Chang, Lue Wu, Jeremy Staffa, Jingwei Ling, Usman A Javid, Yang He, Raymond Lopez-rios, Shixin Xue, Theodore J Morin, et al. Integrated pockels laser. *arXiv preprint arXiv:2204.12078*, 2022.
 - [5] Makoto Kuwata-Gonokami and Kenji Takeda. Polymer whispering gallery mode lasers. *Optical Materials*, 9(1-4):12–17, 1998.

- [6] Lina He, Şahin Kaya Özdemir, and Lan Yang. Whispering gallery microcavity lasers. *Laser & Photonics Reviews*, 7(1):60–82, 2013.
- [7] Farhan Azeem, Luke S. Trainor, Ang Gao, Maya Isarov, Dmitry V. Strekalov, and Harald G. L. Schwefel. Ultra-low threshold titanium-doped sapphire whispering-gallery laser. *Advanced Optical Materials*, n/a(n/a):2102137, 2022.
- [8] Christoph S. Werner, Wataru Yoshiki, Simon J. Herr, Ingo Breunig, and Karsten Buse. Geometric tuning, spectroscopy using whispering-gallery resonator frequency-synthesizers. *Optica*, 4(10):1205–1208, 2017.
- [9] Kishore Padmaraju and Keren Bergman. Resolving the thermal challenges for silicon microring resonator devices. *Nanophotonics*, 3(4-5):269–281, 2014.
- [10] Yuechen Jia, Lei Wang, and Feng Chen. Ion-cut lithium niobate on insulator technology: Recent advances and perspectives. *Applied Physics Reviews*, 8(1):011307, 2021.
- [11] G. Poberaj, H. Hu, W. Sohler, and P. Günter. Lithium niobate on insulator (LNOI) for micro-photonics devices. *Laser & Photonics Reviews*, 6(4):488–503, 2012.
- [12] Jintian Lin, Fang Bo, Ya Cheng, and Jingjun Xu. Advances in on-chip photonic devices based on lithium niobate on insulator. *Photon. Res.*, 8(12):1910–1936, Dec 2020.
- [13] Di Zhu, Linbo Shao, Mengjie Yu, Rebecca Cheng, Boris Desiatov, C. J. Xin, Yaowen Hu, Jeffrey Holzgrafe, Soumya Ghosh, Amirhassan Shams-Ansari, Eric Puma, Neil Sinclair, Christian Reimer, Mian Zhang, and Marko Lončar. Integrated photonics on thin-film lithium niobate. *Adv. Opt. Photon.*, 13(2):242–352, Jun 2021.
- [14] C.-H. Huang and L. McCaughan. 980-nm-pumped Er-doped LiNbO₃ waveguide amplifiers: a comparison with 1484-nm pumping. *IEEE Journal of Selected Topics in Quantum Electronics*, 2(2):367–372, 1996.
- [15] Dominik Brüske, Sergiy Suntsov, Christian E. Rüter, and Detlef Kip. Efficient ridge waveguide amplifiers and lasers in Er-doped lithium niobate by optical grade dicing and three-side Er and Ti in-diffusion. *Optics Express*, 25(23):29374, 2017.

- [16] Dominik Brüske, Sergiy Suntsov, Christian E. Rüter, and Detlef Kip. Efficient Nd:Ti:LiNbO₃ ridge waveguide lasers emitting around 1085 nm. *Optics Express*, 27(6):8884–8889, 2019.
- [17] Zhe Wang, ZhiWei Fang, Zhaoxiang Liu, Wei Chu, Yuan Zhou, Jianhao Zhang, Rongbo Wu, Min Wang, Tao Lu, and Ya Cheng. On-chip tunable microdisk laser fabricated on Er³⁺-doped lithium niobate on insulator. *Optics Letters*, 46(2):380–383, 2021.
- [18] DiFeng Yin, Yuan Zhou, Zhaoxiang Liu, Zhe Wang, Haisu Zhang, ZhiWei Fang, Wei Chu, Rongbo Wu, Jianhao Zhang, Wei Chen, Min Wang, and Ya Cheng. Electro-optically tunable microring laser monolithically integrated on lithium niobate on insulator. *Optics Letters*, 46(9):2127–2130, 2021.
- [19] Wolfgang Sohler. Rare-earth-doped LiNbO₃ waveguide amplifiers and lasers. In Ka Kha Wong, editor, *Integrated Optical Circuits*, volume 1583, pages 110 – 121. International Society for Optics and Photonics, SPIE, 1991.
- [20] Mathew George, Raimund Ricken, Viktor Quiring, and Wolfgang Sohler. In-band pumped Ti:Tm:LiNbO₃ waveguide amplifier and low threshold laser. *Laser & Photonics Reviews*, 7(1):122–131, 2013.
- [21] T. Y. Fan, A. Cordova-Plaza, M. J. F. Digonnet, R. L. Byer, and H. J. Shaw. Nd:MgO:LiNbO₃ spectroscopy and laser devices. *J. Opt. Soc. Am. B*, 3(1):140–148, Jan 1986.
- [22] Ivan S. Grudinin and Nan Yu. Dispersion engineering of crystalline resonators via microstructuring. *Optica*, 2(3):221–224, Mar 2015.
- [23] Simon J. Herr, Yannick Folwill, Karsten Buse, and Ingo Breunig. Self-frequency doubling in a laser-active whispering-gallery resonator. *Optics Letters*, 42(13):2627–2630, 2017.
- [24] Simon J. Herr, Karsten Buse, and Ingo Breunig. Led-pumped whispering-gallery laser. *Photon. Res.*, 5(6):B34–B38, Dec 2017.

- [25] Ingo Breunig. Three-wave mixing in whispering gallery resonators. *Laser & Photonics Reviews*, 10(4):569–587, 2016.
- [26] RS Weis and TK Gaylord. Lithium niobate: summary of physical properties and crystal structure. *Applied Physics A*, 37(4):191–203, 1985.
- [27] E. Diéguez A. Méndez, A. García-Cabañes and J.M. Cabrera. Wavelength dependence of electro-optic coefficients in congruent and quasi-stoichiometric LiNbO₃. *Electronics Letters*, 35:498–499(1), March 1999.
- [28] Yannick Minet, Hans Zappe, Ingo Breunig, and Karsten Buse. Electro-Optic Control of Lithium Niobate Bulk Whispering Gallery Resonators: Analysis of the Distribution of Externally Applied Electric Fields. *Crystals*, 11(3):298, 2021.
- [29] N. MacKinnon, C. J. Norrie, and B. D. Sinclair. Laser-diode-pumped, electro-optically tunable Nd:MgO:LiNbO₃ microchip laser. *J. Opt. Soc. Am. B*, 11(3):519–522, Mar 1994.
- [30] M.L. Gorodetsky and A.E. Fomin. Geometrical theory of whispering-gallery modes. *IEEE Journal of Selected Topics in Quantum Electronics*, 12(1):33–39, 2006.
- [31] Simon J. Herr, Karsten Buse, and Ingo Breunig. Tunable single-frequency lasing in a microresonator. *Optics Express*, 27(11):15351–15358, 2019.